frontiers | Frontiers in Materials

TYPE Original Research
PUBLISHED 15 November 2023
DOI 10.3389/fmats.2023.1234065



OPEN ACCESS

EDITED BY
Daixin Ye,
Shanghai University, China

REVIEWED BY
Muhammad Umar Aslam Khan,
Universiti Teknologi Malaysia, Malaysia
Juliana Silva Ribeiro de Andrade,
Federal University of Santa Catarina, Brazil

*CORRESPONDENCE
Nawshad Muhammad,
nawshad.ibms@kmu.edu.pk

RECEIVED 03 June 2023
ACCEPTED 26 October 2023
PUBLISHED 15 November 2023

CITATION
Farman H, Khan MA, Alamoudi AJ, Sharif F, Alshamrani M, Liaqat S, Rizg WY, Shaik RA and Muhammad N (2023), Fabrication of polymeric composite GTR membrane from eggshell powder, polylactic acid and polyethylene glycol for periodontal application: *in vitro* evaluation.
*Front. Mater.* 10:1234065.
doi: 10.3389/fmats.2023.1234065



# Fabrication of polymeric composite GTR membrane from eggshell powder, polylactic acid and polyethylene glycol for periodontal application: *in vitro* evaluation

Humaira Farman[1], Muhammad Adnan Khan[1], Abdulmohsin J. Alamoudi[2], Faiza Sharif[3], Meshal Alshamrani[4], Saad Liaqat[1], Waleed Y. Rizg[5], Rasheed A. Shaik[2] and Nawshad Muhammad[1]*

[1]Department of Dental Materials, Institute of Basic Medical Sciences, Khyber Medical University, Peshawar, Khyber Pakhtunkhwa, Pakistan, [2]Department of Pharmacology and Toxicology, Faculty of Pharmacy, King Abdulaziz University, Jeddah, Saudi Arabia, [3]Interdisciplinary Research Center for Biomedical Materials, COMSATS University Islamabad, Lahore Campus, Lahore, Punjab, Pakistan, [4]Department of Pharmaceutics, College of Pharmacy, Jazan University, Jazan, Saudi Arabia, [5]Department of Pharmaceutics, Faculty of Pharmacy, King Abdulaziz University, Jeddah, Saudi Arabia

This study aims to fabricate, characterize and evaluate Guided tissue regeneration (GTR) membrane containing eggshell (ES), chlorhexidine (CHX) and polymeric matrix for periodontal application. ES powder ground to size 74 µm was mixed in Polylactic Acid (PLA) and Polyethylene Glycol (70:30 ratios) mixture in 10% and 30% wt to fabricate the membrane and named groups C-10 and C-30. Along with this, 0.25% and 0.5% CHX powder were adsorbed on ES powder and incorporated in PLA and PEG mixture to fabricate drug containing groups C-10CHX and C-30CHX respectively. UTM was used to measure tensile strength, Young's Modulus, and percent elongation of the prepared GTR membrane. Experimental groups containing 10% ES powder (C-10 and C-30) had adequate tensile properties. The percent mass change of the samples was calculated by the change in weight of the samples ($W_d$) from the weight of samples after immersion in phosphate-buffered saline PBS ($W_t$). Contact angle measurement showed that all membranes were found to be hydrophilic (contact angle<90). Groups containing the drug CHX (C-10CHX and C-30CHX) had significant disc diffusion antibacterial activity. Cell viability assay was carried out by Alamar Blue Assay using mouse fibroblasts NIH3T3 and pre-osteoblasts that indicated very good biocompatibility of the groups (C, C-10, C-30, and C-10CHX) while experimental group C-30CHX showed slight cytotoxicity (Cell Viability >70%).

KEYWORDS

**GTR membrane, eggshell powder, chlorhexidine, tensile strength, physical properties, biological properties**

# 1 Introduction

Guided Tissue Regeneration (GTR) is a surgical procedure employed to repair periodontal defects that cannot be effectively treated using conventional methods like scaling, polishing, and root planning. This innovative technique involves the use of a GTR membrane, which acts as a physical barrier to prevent unwanted epithelial and soft tissue cells from encroaching into bony defects (Bokhari et al., 2023a). While the adjacent epithelial cells proliferate rapidly and migrate to the treatment area, bone tissue and the periodontal ligament (PDL) have a slower regenerative process (He et al., 2020). Thus, maintaining space is a crucial aspect of the GTR procedure. First-generation GTR membranes, made of non-biodegradable materials like PTFE (Polytetrafluoroethylene), served as effective physical barriers but necessitated a secondary surgical removal (Abu-Dalo et al., 2022). The introduction of second-generation GTR membranes, composed of biodegradable polymers of natural and synthetic origin, marked a significant advancement, as they eliminated the need for removal surgery (Wang et al., 2016). These biodegradable polymers, such as collagen, chitosan, gelatin, and silk fibroin, offer excellent biocompatibility and biodegradability but may lack mechanical strength and, in some cases, can trigger immune responses (Geão et al., 2019). Polylactic acid (PLA), derived from renewable sources like corn and sugar beets, is an aliphatic polyester known for its exceptional biodegradability, making it environmentally friendly (Golińska et al., 2021). Polyethylene Glycol (PEG), often used as a plasticizer, enhances the ductility and film-forming properties of PLA, making it a versatile biomaterial (Ensing et al., 2019). Biodegradable polymers are also gaining attention for their potential in controlled drug delivery (Yang et al., 2022). This study explores the fabrication of a novel GTR membrane by incorporating eggshell (ES) powder as a cost-effective source of bio-CaCO3 in a polymer matrix, improving biocompatibility, wettability, and water sorption without compromising tensile strength. Additionally, chlorhexidine (CHX) is added to the membrane for sustained antibacterial release, reducing the risk of infection at the GTR site.

Eggs are a staple in many cultures and are consumed worldwide daily. Eggshell waste is considered useless and is a large contributing factor to pollution as they are mostly dumped into landfills which have filled capacities and cause harmful environmental factors. Their management is problematic since it is one the most ample sources of waste due to its abundance. Efforts are being made to turn it into something useful for different applications (Skórczewska et al., 2022). Since eggshells are composed of ninety-five percent inorganic material mainly calcium carbonate ($CaCO_3$), it can have tremendous applications and benefits as a cost-effective source of calcium and its compounds. $CaCO_3$ can be converted into hydroxyapatite which is the main component of bone and teeth. $CaCO_3$ is also osteoconductive meaning it allows osteoblasts to proliferate on its surface but for bone healing to take place, the surface needs to be osteo-inductive. Bone regeneration relies on osteoinductive surfaces to actively recruit progenitor osteoblast cells and differentiate them into osteoblasts for bone formation and bone maturation. $CaCO_3$ also has proven bioactivity by releasing calcium ions $Ca^{2+}$ which stimulate pre-osteoblasts to differentiate into mature osteoblasts and promote bone regeneration *in vivo* (Masoudi Rad et al., 2017). $CaCO_3$ also acts as a buffer and is beneficial in neutralizing lactic acid produced by PLA by the process of hydrolytic scission. Since $CaCO_3$ is a mineral and can release calcium, it acts with the acid and acts as a buffer which is another beneficial property of the material. $CaCO_3$ is also very bioresorbable and increases the biodegradability of PEG since PEG has quite a slow biodegradation rate (Sam et al., 2015). $CaCO_3$ increases the toughness of PLA and PEG based membranes which are reduced by the sift PEG but it can affect its tensile strength which needs to be evaluated. Tensile strength is of utmost importance for GTR membranes not only in their manufacturing process but also in clinical manageability (Lopez-Berganza et al., 2017). Images from scanning electron microscopy (SEM) have shown that eggshell powder exhibited better incorporation with polymers than when synthetic calcium carbonate was used as a filler material (McGauran et al., 2020).

This study focused on the fabrication of a novel GTR membrane by adding ES powder as a cost-effective source of bio-$CaCO_3$ in a polymeric matrix. The addition of CaCO3 in the form of ES powder to improve the biocompatibility, wettability, and water sorption of the PLA-PEG polymer blend of the GTR membrane without affecting its tensile strength. Good wettability and higher water sorption of the GTR membrane help in better uptake ability and drug release which promotes cell adhesion and proliferation. CHX as an antibacterial agent was added for slow and sustained release to reduce the risk of infection in the GTR membrane and bone healing sites.

# 2 Materials and methods

## 2.1 Chemicals

Polylactic acid (PLA) (MW: 60,000), polyethylene glycol (PEG) (MW: 4,500), and chlorhexidine (CHX) (≥99.5%) were obtained from Sigma-Aldrich, United States. Chloroform (Chl) was supplied by EMPARTA ACS, United States, and Golden misri hen eggs were purchased from the local market in Peshawar, Pakistan.

## 2.2 Grinding of eggshells (ES)

Eggs were cracked open and eggshells (ES) were collected in a separate utensil. The ES was cleaned in a sink under running water at 35°C for 5 min to remove impurities. ES were laid in a disinfected tray and air dried for 24 h to facilitate the process of grinding. Dried eggshells were then manually crushed before grinding in a grinder into fine powder. The powder was then passed through a number 200 stainless steel laboratory sieve (74 μm diameter) to obtain a fine powder of 74 μm grain size. It was then collected in an airtight glass jar and stored in a fridge at 4°C to be utilized for sample preparation (Shiferaw et al., 2019).

## 2.3 Preparation of the membranes

The solvent casting method was used to prepare five groups of the GTR membranes. Group 1 (C) was prepared by mixing PLA pellets and PEG flakes in 70% and 30% ratios and dissolving in 99.9% pure Chl solvent to prepare a 5% solution. Group 2 (C-10)

and group 3 (C-30) were prepared by mixing 10% and 30% ES powder in the polymer mixtures respectively. Groups containing drug group 4 (C-10CHX) and group 5 (C-30CHX) were prepared by adding 0.25% and 0.5% CHX powder in the above mentioned polymers and ES powders. The mixtures were stirred on a magnetic stirrer heated to 50 °C at 800rpm until the polymers and CHX were dissolved into a homogenous solution. The solutions were then poured into glass Petri dishes and covered with an inverted funnel plugged with loose cotton for slow evaporation for 24 h. After 24 h, the membranes were placed in a hot air oven at 60°C. After 4 h, the Petri dishes were taken out from the oven and the dried membranes were peeled off from the Petri dish and stored in a sterile zip lock bag for further analyses.

## 2.4 Characterization and analyses

### 2.4.1 FTIR

Chemical analysis for functional group identification of the ES powder and GTR membranes was performed using Fourier transform infrared spectroscopy (FTIR, Thermo Scientific Nicolet 6700) over a wavelength range from 400 to 4,000 $cm^{-1}$ at a resolution of 4 $cm^{-1}$.

### 2.4.2 Scanning Electron Microscopy (SEM)

The surface and cross-sectional morphologies of the fabricated GTR membranes were studied by scanning electron microscopy. For the cross-sectional area, each sample was prepared by the "direct freeze-fracture method" (Cryo-Snap). GTR membranes were cut into (8 × 8) mm strips and immersed into freshly poured liquid nitrogen for a few seconds. Once the membranes became brittle, the samples were taken out and manually broken. The samples were examined using the scanning electron microscope; Model: L1600300, England. Images of the surface and cross-sectional areas were captured at various magnifications.

### 2.4.3 X-ray Diffraction (XRD)

ES powder was analyzed by the X-ray diffractometer. Scans were taken in the 2θ range ≈20°–80°; with a step size of 0.02° for crystallinity and phase identification of the ES powder.

## 2.5 Mechanical properties

The mechanical properties (tensile strength, Young's modulus, and elongation at break) of the five groups of GTR membranes were evaluated by using a universal testing machine (UTM) (electrodynamics fatigue testing machine, Walter + bai AG, Switzerland). Three specimens (n = 3) from each group were cut into rectangular strips (30 mm × 5 mm) and tested. The crosshead speed was set at 1 mm/min. The results were calcuted as average value of the triplicate (He et al., 2019).

## 2.6 Mass change

Mass change as a result of the water sorption capacity of the GTR membranes was measured in triplicate. Three samples from each of the five groups ($n$ = 3) were prepared by cutting the GTR membranes into (10 × 10) mm dimensions. The dry weight of the GTR samples was measured by digital balance and noted down. After measuring the dry weight, the membranes were immersed in PBS for different time intervals (30 min, 1h, 3h, 6h, 24 h, and 10 days) to determine the percent mass change using the formula

$$\textbf{Water intake}\ (\%) = \textbf{Wt} - \textbf{Wd}/\textbf{Wd} \times \textbf{100}$$

## 2.7 Antibacterial studies

The *in vitro* antibacterial effect of the fabricated GTR membranes was examined against *Enterococcus*. faecalis (*Enterococcus faecalis* ATCC 29212) by "disk diffusion method." With the help of a sterile swab, E. facecalis inoculum was taken and spread over a nutrient agar (NA) plate by "Surface Streaking Method" to form colonies of the strain and incubated at 37°C for 24 h. Using an inoculation loop, colonies of E. faecalis were picked up from the NA plate and transferred to a sterile test tube containing distilled water. The bacterial suspension was then visually compared to the 0.5 McFarland standards estimating the bacterial density. Mueller Hinton Agar (MHA) media was made in distilled water and sterilized at 121 ℃ for 25 min. The MHA broth was poured into Petri dishes. The experiment was performed in triplicate ($n$ = 3). Three small pieces from each group of the five samples of GTR membrane were cut and placed on the prepared Petri dishes and incubator at 37°C. After 48 h of incubation, Petri dishes were taken out and the mean inhibition diameters around each disk of the samples were carefully measured (Joy Sinha et al., 2017).

## 2.8 Contact angle

Sessile drop method analysis was performed to measure the wettability of the five groups of the GTR membranes. A droplet of distilled water (3 μL) was horizontally dropped on the surface of the GTR membrane with the help of a micropipette. Images were taken and the software ImageJ (plugin Contact Angle) was used to determine the contact angle of the water drop formed at the interface with the sample (Grundke et al., 2015).

## 2.9 Cytotoxicity

The cytotoxicity of ES powder, control (C), and experimental groups (C-10, C-30, C-10CHX, C-30CHX) was determined by performing Alamar blue assay using NIH3T3 mouse embryonic fibroblasts and MC3T3 pre-osteoblasts cell lines (American Type Tissue Culture CRL-1658 and CRL 2594). The biocompatibility of a biomaterial with MC3T3 can imply their osteogenic potential *in vivo* conditions. The NIH3T3 fibroblasts and MC3T3 were cultured using Alpha-modified Eagle's medium (Biosera, United Kingdom), 10% FBS, and 1% Penicillin/Streptomycin (Pen/Strep). Three samples from each group ($n$ = 3) were first sterilized with 70% ethanol and then washed with PBS three times (15 15-min intervals) before the experiment. After 24 h, the medium was replaced by Alamar blue reagent and incubated at 37°C for

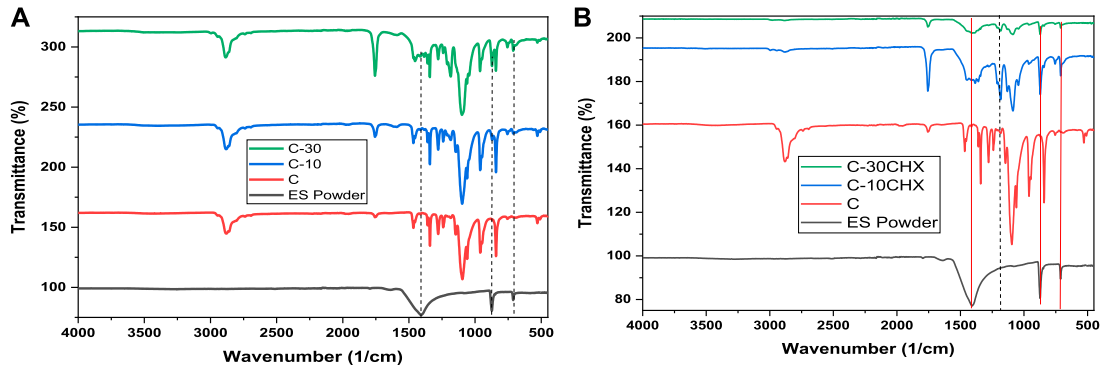


FIGURE 1
FTIR of **(A)** pure ES powder and GTR groups C, C-10, and C-30 **(B)** ES powder and GTR groups C, C-10CHX, and C-30CHX.

4 hours. After 4h, the absorbance was measured by the micro-plate reader at 570 nm. The cell viability results were expressed as average absorbance values of the triplicates using the formula

$$\%\text{Cell Viability} = (\text{sample absorbance})/(\text{cell control absorbance}) \times 100$$

# 3 Results and discussion

## 3.1 FTIR

FTIR analysis was performed in this study to confirm the presence of ES powder and CHX in the fabricated GTR membranes (Qasim et al., 2021a). Figure 1A demonstrates the characteristic peaks of ES powder and GTR groups C, C-10, and C-30. Stretching vibrations of ES powder belonging to C–O and O–C–O linkages have been observed at 1,404 and 874 $cm^{-1}$ respectively. Another small sharp peak was observed at 704$cm^{-1}$ representing the absorbance by the Ca-O bond (Akram et al., 2021). In the FTIR graph, an increase in the intensity of the characteristic peak is indicative of an increase in the amount of the corresponding constituent. Therefore, C-10 containing 10% ES powder has lower peaks present than C-30 containing 30% ES powder while in the control group (C), they are absent altogether since there is no ES powder in group C. Similarly, in Figure 1B, it would be seen that group 1(C) did not present with a characteristic peak associated with C-N bending of CHX at 1,119 cm, $^{-1}$ while these have been identified for group C-10CHX and C-30CHX (Priyadarshini et al., 2017). These findings confirm the presence of ES powder and CHX in the experimental groups of GTR membranes.

## 3.2 SEM

Scanning electron microscopic evaluation of the surface morphology of the five groups of GTR membranes at ×250 magnification has been shown in Figure 2A. Group 1 (C) showed the conglomerated appearance of PLA and PEG blend with numerous voids which were typical of a GTR membrane surface fabricated by the solvent casting method (Ghosal et al., 2018). With the addition of ES filler, there was a marked decrease in surface porosities in the experimental groups (Figures 2B–E). The addition of CHX as a drug also had significant effect on surface characteristics. The SEM images showed aggregates of ES filler and CHX dispersed on the surface of the GTR membranes, which contributed to the increase in the surface roughness but decreased the surface voids (Ghafoor et al., 2020). Surface roughness of a membrane plays a critical role in cell adhesion and proliferation as the osteoblasts are reported to be sensitive to roughness of the surface of a material. The reason could be explained by the increased surface area of the material for serum proteins to act for a higher percentage of cell adhesion than their polished counterparts (Li et al., 2012).

A homogenous cross sectional area structure was observed by SEM in Figure 3. Group 1 (C) showed porous and dense morphology. The experimental groups (C-10, C-30, C-10CHX, and C-30CHX) also showed similar morphology but were denser with fewer voids present which suggests that the filler components ES powder and CHX were uniformly distributed throughout the samples (Wu et al., 2022).

## 3.3 XRD

The XRD pattern of experimental ES powder is shown in Figure 4. Through X-ray diffraction, data from ES powder was collected at 10–70° in the 2-theta range. The ES powder showed characteristic peaks of $CaCO_3$ at (012), (110), (104), (006), (110), (113), (202), (024), (211), (122), (244), (300), (012) at 23.1°, 29.37°, 35.9°, 39.3°, 43.2°, 47.5°, 48.5°, 57.4°, 48.5°, 57.4°, 58.3° and 60.86°,64.77° and 67.97° respectively. The diffraction peak marked at approximately 34.30 (2-theta) indicates that the ES powder contains a calcite crystalline structure similar to the reported data of $CaCO_3$ (Al-Jaroudi et al., 2007). The XRD analysis of ES powder revealed the existence of $CaCO_3$ in the thermodynamically stable calcite phase as a major component of the powder. The presence of more than 90% $CaCO_3$ having rhombohedral crystal alignment was proved through this analysis. Therefore, ES powder as a natural source of $CaCO_3$ was utilized for the fabrication of novel GTR membranes in this study (Wei et al., 2004).

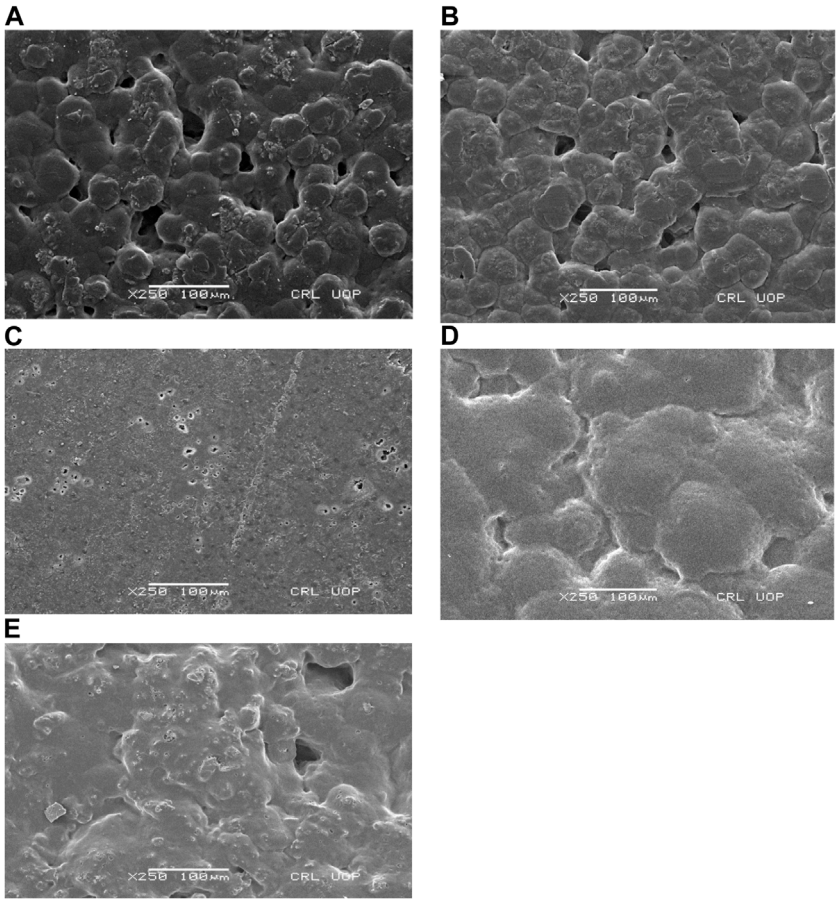


FIGURE 2
SEM images of the surface at 250 magnification of **(A)** group 1 **(C)**, **(B)**, group 2 (C-10), **(C)** group 3 (C-30), **(D)** group 4 (C-10CHX), and **(E)** group 5 (C-30CHX).

## 3.4 Tensile tests

### 3.4.1 Tensile strength

The mean tensile strength of all the GTR groups is shown in Figure 5. Maximum mean tensile strength was recorded for Group 4 (10.22 ± 1.1) MPa followed by Group 1 (8.99 ± 0.24 MPa). The lowest tensile strength was observed for group 5 (3.15 ± 0.91 MPa). Statistical analysis showed a significant difference in results ($p$ = 0.000) with all the groups, i.e., within the control and the experimental groups. Among the groups, group 1(C) has shown a significant difference with group 3 (C-30) with a $p$-value of 0.000 and 5(C-30CHX) with a $p$-value of 0.000. Group 3 has a significant difference in results with group 2(C-10) ($p$ = 0.001) and group 4 (C-10CHX) ($p$ = 0.000). Interest in improving the tensile properties of a GTR membrane has increased over time for functional integrity, proper handling, suturing, and the enhancement of biological space for the continued release of cells and growth factors, drugs, etc. When comparing the groups, group 4(C-10CHX) membranes showed the highest tensile strength at (10.22 ± 1.1 MPa) which is comparable to commercial GTR membranes. The second highest value of tensile strength was recorded for group 1 (C) without any ES filler. The lowest value recorded was for the highest amount of ES filler in group 5 (C-30CHX) which indicates that while ES powder in a small concentration improves the tensile strength, higher ratios are related to decreased tensile strength which is undesirable in GTR membranes (Gao et al., 2022). These results are consistent with a study conducted by Kai Zhang et al. in which hydroxyapatite was incorporated into the chitosan matrix for the fabrication of a GTR membrane. The tensile strength and elongation at break percentages of the GTR membranes decreased as the hydroxyapatite content in the chitosan matrix increased (Zhang et al., 2010).

### 3.4.2 Young's modulus

Maximum mean Young's Modulus was observed for GTR group C-10CHX (644.42 ± 104.14) MPa followed by group C (523.17 ± 29.0) MPa. The lowest value was observed for group C-30CHX (374.55 ± 123.96) MPa. With a $p$-value of 0.06, the difference was not significant among the five experimental groups. The Young's modulus (E) should fall within an acceptable range because an excessively large value of Young's Modulus would hinder manageability during surgical procedures and cause tissue damage. On the other hand, an insufficient Young's Modulus would compromise space maintenance.

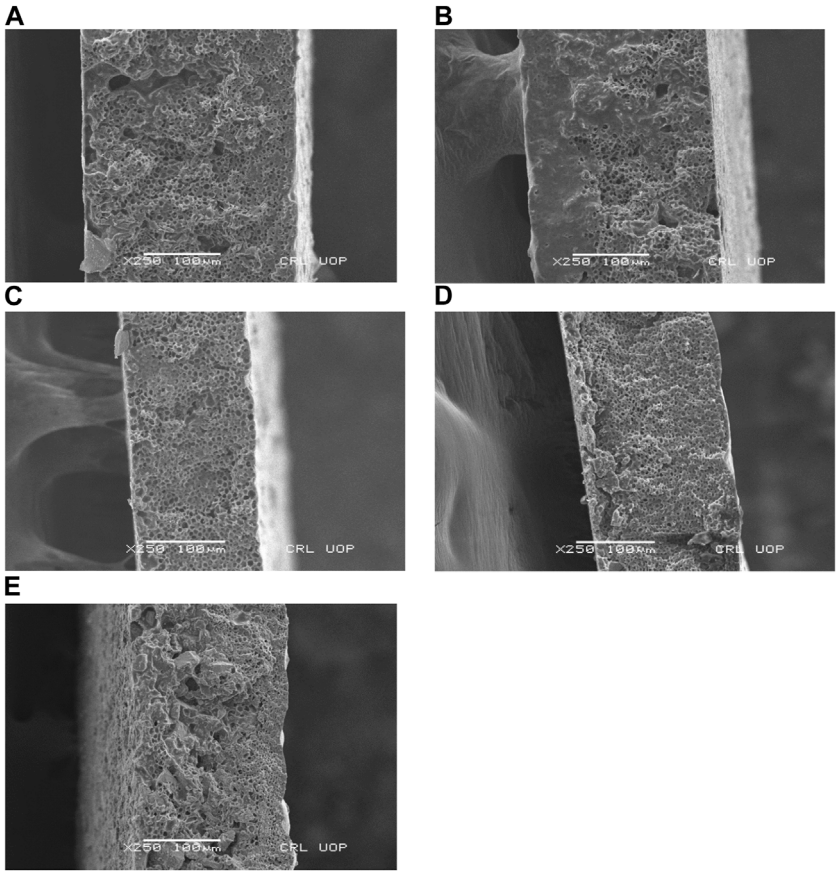


FIGURE 3
SEM images of the cross-sectional area of **(A)** group 1 **(C)**, **(B)**, group 2 (C-10), **(C)** group 3 (C-30), **(D)** group 4 (C-10CHX), and **(E)** group 5 (C-30CHX).

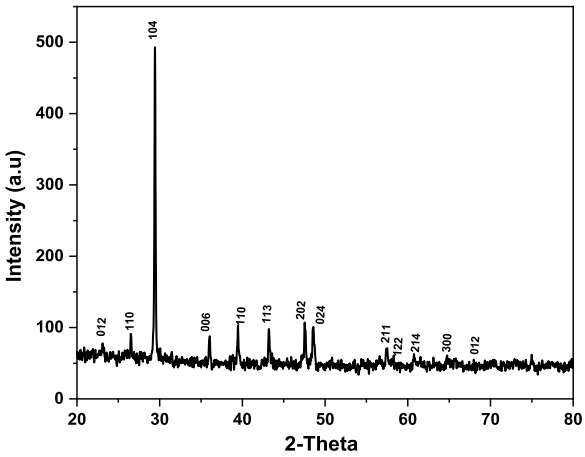


FIGURE 4
X-ray diffraction analysis of ES Powder.

Commercial GTR membranes have Young's Moduli ranging from 30.6 to 700 MPa approximately so comparatively, ES modified PLA and PEG based GTR membranes were on the stiffer side (Milella et al., 2001).

### 3.4.3 Percent elongation

The highest percent elongation was observed for group C at (5.76 ± 3.91) % followed by group 4(C-10CHX) at (4.83 ± 0.93) %. The lowest value was observed for group 3 (C-30) at (1.46 ± 1.40) %. One way ANOVA test was not significant for percent elongation among the five groups ($p$ = 0.126). Elongation at break should be increased for a GTR membrane so that it can bear forces and undergo deformation before breakage. Normally, increasing tensile strength results in decreasing percent elongation. Ghosal et al. (2018) compared the mechanical properties of solvent cast poly (ε-caprolactone) (PCL) *versus* electrospun membranes and concluded that the electrospun membranes had excellent percent elongation than those of solvent cast ones. The reason was explained by the stretching of the aligned fibers formed during the electrospinning technique (Ghosal et al., 2018). Elongation also depends on whether the material was tested in dry or wet conditions. Elongation increases when the GTR membrane is wet (Susanto et al., 2019), on the contrary, tensile strength decreases when the GTR membrane is used wet, unlike the tensile strength which decreases with moisture (Dimitriou et al., 2012). From these results, it can be inferred that each of the five groups presented great results owing to application in GTR surgery except group 5(C-30CHX) which presented undesirable tensile values for clinical conditions. For instance, if stronger support is needed in applications like large bone defects or bone augmentation, group 4(C-10CHX) membrane can be

10.3389/fmats.2023.1234065

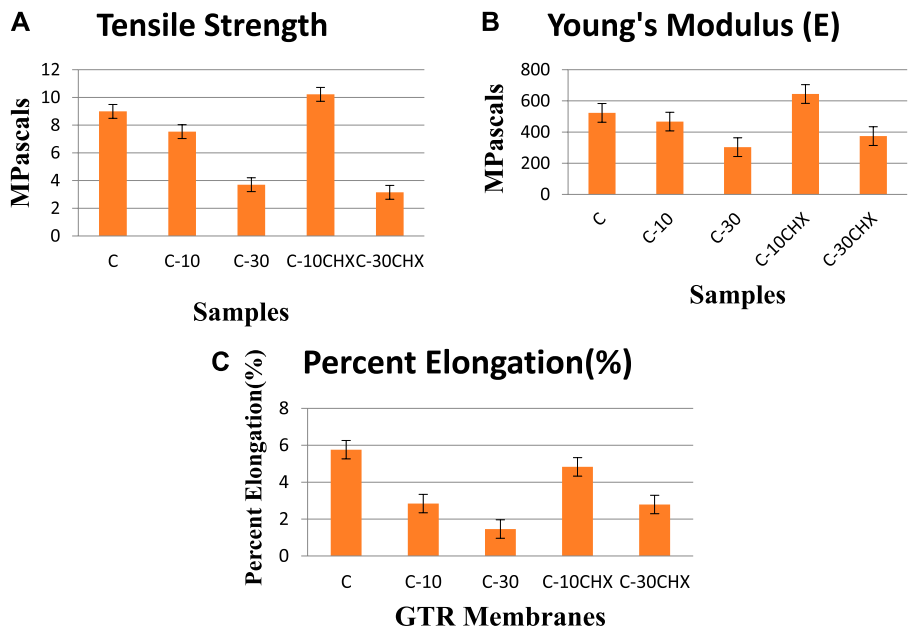


FIGURE 5
Bar charts representing **(A)** mean Tensile Strength (MPa) **(B)** mean Young's modulus (MPa) and **(C)** mean percent elongation of the five groups of GTR membranes.

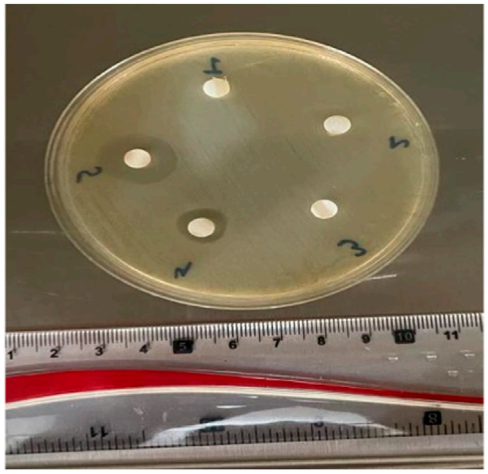

FIGURE 6
Zones of inhibition (mm) for GTR membranes incubated in MHA media for 48 h against E. faecalis suspension.

considered ideal for the applications requiring ultimate strength along better manageability (elongation at break), to grant the membranes with proposed mechanical properties and fulfilling any kinds of clinical demand (Lenzi et al., 2012).

## 3.5 Antibacterial test

The mean diameters of the zone of inhibition (mm) after 48 h are represented in Figure 6. The highest value for the zone of inhibition was observed in group 5(C-30CHX) (17.3 ± 0.58 mm) followed by group 4 (C-10CHX) (10 ± 1 mm as tabulated in Table 1). There were no zones of inhibitions found in Groups 1(C), group 2 (C-10), and group 3(C-30). Statistical analysis showed a significant difference ($p \leq 0.05$) between groups containing CHX; group 4(C-10CHX0 and group 5(C-30CHX) and other groups without the drug; group 1(C), group 2 (C-10) and group 3 (C-30). In the experimental groups containing CHX, group 5 showed a significant difference from group 4 ($p < 0.000$).

Oral cavity harbours a plethora of microorganisms like bacteria, viruses, fungi and protozoa Contamination by bacteria is one of the most significant factors leading to a reduced outcome in alveolar bone regeneration using the GTR technique. Enterococci particularly *E. faecalis* has shown to play an important role in the progression of periodontal diseases which might negatively impact the progress of the regenerative therapy (Bhardwaj et al., 2020) CHX is a broad spectrum antimicrobial effective against Gram positive bacteria, Gram negative bacteria and fungi. Therefore, imparting antibacterial property to a GTR membrane could be extremely beneficial for successful GTR therapy (Bhardwaj et al., 2020; Abdo et al., 2023). In this study, the antibacterial activity of the specimens against *E. faecalis* was studied *in vitro* using disc diffusion methods. After 48 h of incubation, the maximum zone of inhibition was seen around group 5 (C-30CHX) containing the highest amount of CHX (0.5%) followed by group 4 (C-10CHX) containing 0.025% of CHX while there were no zones of inhibition was noticed around groups that did not contain CHX (C, C-10, and C-30). These results indicated that increasing the concentration of CHX increased the antibacterial potential of the GTR membrane which is following a study in which increasing the concentration of CHX doubled the antibacterial activity of a collagen based GTR membrane (Khan et al., 2022a).

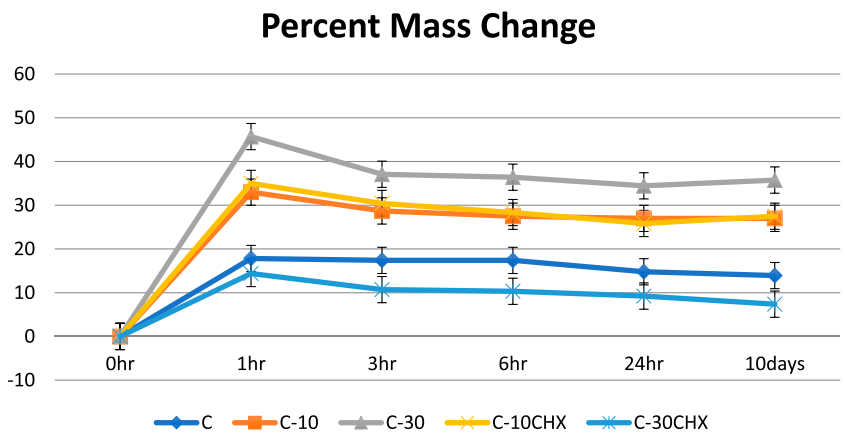


FIGURE 7
Percent mass gain of five groups of GTR membrane over 10 days time period *X*-axis represents time intervals and the *Y*-axis represents the mass change in percentage (%).

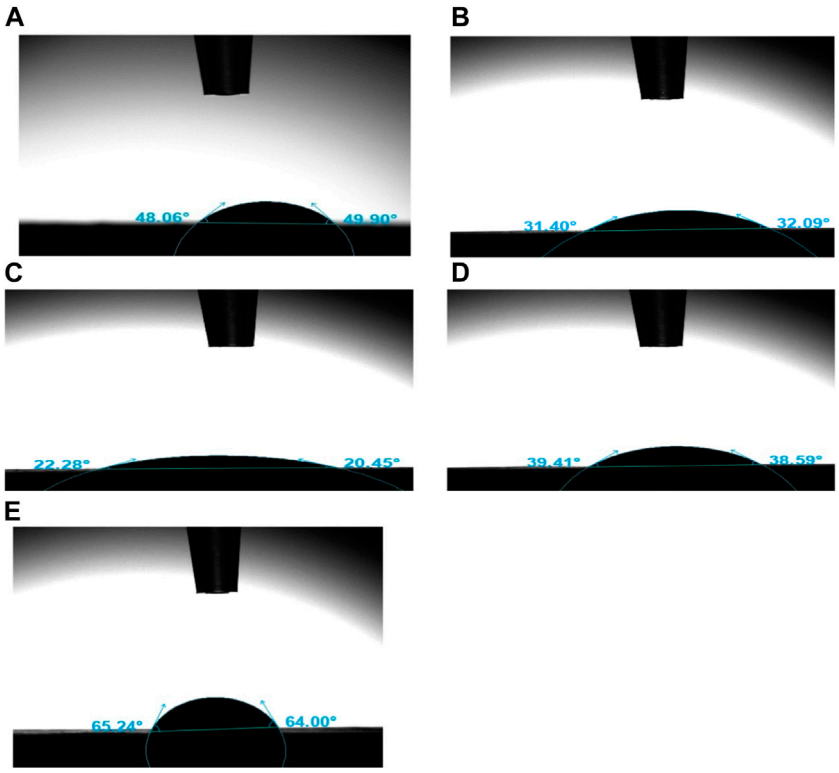


FIGURE 8
Contact Angles formed by water droplets with GTR groups **(A)** C, **(B)** C-10, **(C)** C-30, **(D)** C-10CHX, **(E)** C-30CHX.

## 3.6 Mass change

The mean percent mass change after 1 h as shown in Figure 7 was highest for group 3 (C-30) which is consistent with literature that composites with higher loading of ES powder show more water sorption. The presence of a high level of $CaCO_3$ in the ES powder can absorb more water, so it increases the water absorption as the filler increases (Farahana et al., 2015). This is in contrast to a study in which hydroxyapatite was used as a filler material. Swelling decreased as the amount of HA increased in the samples (Qasim et al., 2021b). Group 5 (C-30CHX) containing the same amount of ES filler as group 3 (C-30) but also containing CHX has the lowest percent mass increase among the groups after 1 h. Water sorption depends mainly on two factors; the hydrophilicity/hydrophobicity of the material and the extent of porosity. Hence, the reduction may be

due to CHX filling up any voids present making it more impermeable and hence less water sorption and mass increase (Vasudevan and Chan Wei, 2020) Or it could also be attributed to CHX forming a surface coating on the ES powder due to its adsorbent property. Since CHX is significantly less hydrophilic than $CaCO_3$, the mass change was lowest for C-30CHX. Group 5 (C-30CHX) containing the maximum amount of drug CHX has the lowest water absorption. This could be explained by the less porous structure ofgroup 5 (C-30CHX) resulting in lesser swelling or CHX forming a surface coating on the ES powder due to the adsorbent nature of the ES powder particles (Khan et al., 2022b).

## 3.7 Contact angle

The results of the sessile drop method technique showed that the contact angle of the fabricated GTR membrane was lowest for group C-30 at 22.29° (tabulated in Table 2). Contact angles recorded for all groups were below 90 indicating hydrophilic surfaces (Latthe et al., 2014).

GTR membranes should be fairly hydrophilic for water since it is the conveying medium to carry nutrients to the bony area that needs to be regenerated. Hydrophilic surfaces are also reported to enhance cellular attachment, proliferation, and elongation of the osteoblasts and other cells (Brum et al., 2021). However, too high water levels in the GTR membrane can soften the membrane and compromise its mechanical properties (Fernandes et al., 2020).

The results of this study showed that all five groups of GTR membranes were hydrophilic (contact angle <90°) (Ahmad et al., 2018). Experimental group 3(C-30) had the smallest contact angle (22.2°) indicating very strong hydrophilicity as shown in Figure 8. This can be explained by the presence of high amount of CaCO3 in the sample. $CaCO_3$ is a hydrophilic mineral and non-toxic substance that has been widely used as a functional filler in biomaterials for improving aspects like mechanical properties and bioactivity (Shamsuri and Sumadin, 2018). These results are consistent with studies in which bioglass and hydroxyapatite were used as the inorganic filler. Increasing the amount (weight percentage) of bioglass and hydroxyapatite in a polymeric matrix increased the wettability of the GTR membranes (Soltani Dehnavi et al., 2018; Zimina et al., 2020).

Group 5(C-30CHX) containing 30% ES filler same as group 3(C-30) has a much higher contact angle (22.29° vs. 64.6°) which could be explained by two factors. One is CHX being less hydrophilic than $CaCO_3$ and the other is the inherent adsorbent property of $CaCO_3$ in the form of ES powder. ES powder is an excellent adsorbent material and CHX may have formed a surface coating over the ES powder particles, thus increasing the value of Contact Angles in groups 4 and 5. Thus, incorporation of different concentration of ES powder results in different types of GTR membranes with varying levels of wettability and contact angle of the membranes (Khan et al., 2022c).

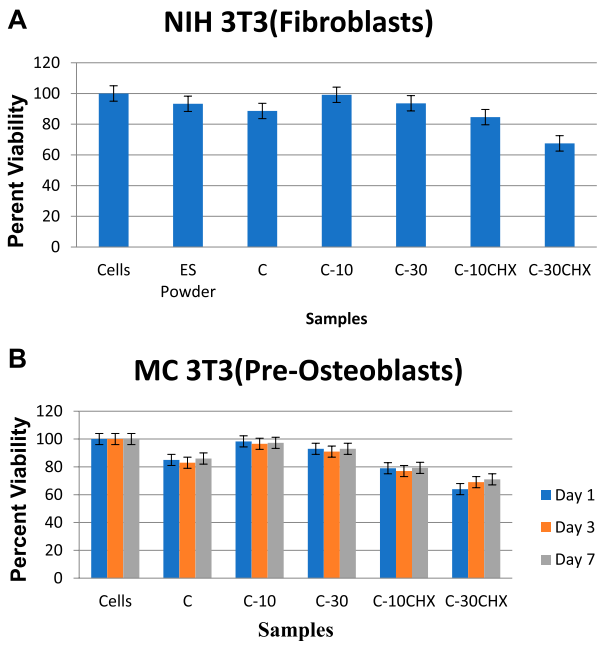


FIGURE 9
Cell viability of cells, ES Powder, control and 5 groups of GTR membrane on **(A)** NIH 3T3 (Fibroblasts) and **(B)** MC 3T3 (Pre-Osteoblasts).

## 3.8 Cytotoxicity

### 3.8.1 NIH3T3 Fibroblasts

The results of the Alamar Blue Assay are presented in Figure 9. Results indicate that ES powder and experimental groups (C, C-10, C-30, and C-10CHX) had no cytotoxic effects on NIH 3T3 fibroblasts at 24 h (all values > 70%) (Cannella et al., 2019a). Experimental group C-10 showed the highest level of cell viability (99%) to cells of the control indicating excellent biocompatibility. Experimental group C-30CHX containing 0.5% CHX showed slight toxicity at 67.3% (<70%).

The ANOVA analysis of the data indicated significant differences among groups for cell viability percentages ($p < 0.000$). The post-hoc-Tukey analysis showed a significant difference in all the groups (ES Powder, C, C-30, C-10CHX, and C-30CHX) concerning the control cells except C-10 ($p = 0.622$) indicating very high cell viability percentage for group C-10.

### 3.8.2 MC3T3

The results of the Alamar Blue Assay are presented in Figure 9B. Results indicate that the ES powder and experimental groups (C, C-10, C-30, and C-10CHX) had no cytotoxic effects on MC3T3 fibroblasts at 1,3, and 7 days (all values > 70%). Experimental group C-10 showed the highest level of cell viability (99%) to cells compared to the cells indicating excellent biocompatibility. Experimental group C-30CHX containing the highest amount of CHX showed slight toxicity at 67.3% (<70%).

**TABLE 1 Mean diameter of Zone of Inhibitions of five groups of GTR membrane.**

| Groups | Zone of inhibition (mm) |
|---|---|
| C | 0 |
| C-10 | 0 |
| C-30 | 0 |
| C-10CHX | 9.33 ± 1.26 |
| C-30CHX | 17.66 ± 1.26 |

**TABLE 2 Contact Angles formed by GTR membranes of all groups.**

| Groups | Contact angle (°) |
|---|---|
| 1(C) | 49.23 |
| 2(C-10) | 30.11 |
| 3(C-30) | 22.29 |
| 4(C-10CHX) | 39.09 |
| 5(C-30CHX) | 64.6 |

There was no significant difference between the untreated cells and groups C-10 and C-30 ($p = 0.0916$) indicating that ES-modified GTR membranes have osteogenic potential and promote osteogenic differentiation of the MC3T3 cells. However, here C-10-CHX as well as C-30-CHX had cell viability less than 80% which shows the negative effect of CHX present in the GTR membranes. These results are consistent with the results from NIH-3T3 cells where group 5 (C30CHX) showed cytotoxicity and hindered cell proliferation compared to the cells.

A biomaterial is considered to be cytotoxic if the cell viability percentage is below 70% (Cannella et al., 2019b). All the groups except C-30CHX showed excellent biocompatibility. These results are consistent with a study that incorporated hydroxyapatite and bioglass into PCL in which cell viability increased with small quantities of these bioactive materials. But unlike ES powder, their cell viability percentage dropped with an increase in the filler amount (Sunandhakumari et al., 2018). This phenomenon can be attributed to the fact that synthetic hydroxyapatite and bioglass are less biocompatible than natural inorganic materials like ES powder (Reddy et al., 2021). In this respect, a novel GTR membrane with ES filler has better biocompatibility in comparison to synthetic inorganic fillers like hydroxyapatite and bioglass. Hence, the addition of ES results in the alteration of the physiochemical characteristics of the GTR membrane supporting biocompatibility and cell viability and confirming the biocompatible nature of the ES powder (Aslam Khan et al., 2021).

Group 5(C-30CHX) containing 0.5% CHX showed the highest levels of cytotoxicity (<70%) among the GTR membranes which are following a study that proved that fibroblasts, myoblasts, and osteoblasts exposed to CHX in concentration ≥0.02% had cell survival rates of less than 6% in comparison to untreated controls. The clinically used concentration of CHX which is usually (2%) in mouthwashes permanently halts cell migration and significantly reduces the survival of *in vitro* cells (Liu et al., 2018). ES powder and all the other GTR membranes had fair biocompatibility with mouse fibroblasts NIH 3T3 and MC 3T3. Group C-10 presented excellent biocompatibility with no significant difference concerning the control cells. This shows higher viability of membranes synthesized with ES Powder (C-10 and C-30) and lower viability of drug containing membranes (C-10CHX and C-30CHX). This is consistent with a study conducted by Thomas et al. in which they concluded that CHX is toxic in even the smallest concentration (0.05%) against HeLa cells while tetracycline showed fair biocompatibility when incorporated into the GTR membrane (Thomas et al., 2012).

## 4 Conclusion

The Eggshell and polymers were homogenously blended to obtain the desired GTR membrane to repair periodontal defects. FTIR analysis confirmed the presence of $CaCO_3$ and CHX in the ES and CHX-modified GTR membranes. SEM analysis has revealed conglomerated and porous surface morphology of the GTR membranes. The XRD analysis identified the crystalline structure and the inorganic constituent of ES powder. The GTR membranes containing 10% of ES powder (C-10 and C-10CHX) had adequate tensile strength while GTR membranes with 30% ES powder (C-30 and C-30CHX) had inferior tensile properties than control (C) and experimental groups C-10 and C-10CHX. Adding ES powder to PLA and PEG based GTR membrane increased the membrane's mean percentage mass change after 10 days of immersion in PBS. Also, the addition of ES powder increased the hydrophilicity of PLA and PEG based GTR membrane. CHX addition to PLA and PEG based GTR membrane improved the membrane's antibacterial potential against *E. faecalis* after 48 h of incubation. Moreover, ES filler improved the biocompatibility of PLA and PEG based GTR membranes. Hence the prepared GTR membrane has adequate tensile strength, optimum wettability, excellent biocompatibility, and antibacterial potential to be utilized for periodontal application. In conclusion, group 4 (C-10CHX) containing 10% ES powder by weight has adequate tensile properties along with excellent physical properties and biocompatibility and can be successfully used in clinical settings while groups containing 30% ES powder (C-30 and C-30CHX) proved to be too brittle for clinical application due to high content of inorganic filler.

## Data availability statement

The original contributions presented in the study are included in the article/supplementary material, further inquiries can be directed to the corresponding author.

## Author contributions

HF and MK: write up and methodology AA, MA, and WR: Data analysis and funding SL, FS: experimental and review, RS: Analysis, NM; supervision. All authors contributed to the article and approved the submitted version.

## Funding

This research work was funded by Institutional Fund Projects under grant no. (IFPIP:1286-166-1443). The authors gratefully acknowledge technical and financial support provided by the Ministry of Education and King Abdulaziz University, DSR, Jeddah, Saudi Arabia.

## Acknowledgments

The authors gratefully acknowledge technical and financial support provided by the Ministry of Education and King Abdulaziz University, DSR, Jeddah, Saudi Arabia.

## Conflict of interest

The authors declare that the research was conducted in the absence of any commercial or financial relationships that could be construed as a potential conflict of interest.

## Publisher's note

All claims expressed in this article are solely those of the authors and do not necessarily represent those of their affiliated organizations, or those of the publisher, the editors and the reviewers. Any product that may be evaluated in this article, or claim that may be made by its manufacturer, is not guaranteed or endorsed by the publisher.

## References

Abatan, O. G., Alaba, P. A., Oni, B. A., Akpojevwe, K., Efeovbokhan, V., and Abnisa, F. (2020). Performance of eggshells powder as an adsorbent for adsorption of hexavalent chromium and cadmium from wastewater. *SN Appl. Sci.* 2 (12), 1996. doi:10.1007/s42452-020-03866-w

Abdo, V. L., Suarez, L. J., de Paula, L. G., Costa, R. C., Shibli, J., Feres, M., et al. (2023). Underestimated microbial infection of resorbable membranes on guided regeneration. *Colloids Surfaces B Biointerfaces.* 226, 113318. doi:10.1016/j.colsurfb.2023.113318

Abu-Dalo, M. A., Al-Atoom, M. A., Aljarrah, M. T., and Albiss, B. A. (2022). Preparation and characterization of polymer membranes impregnated with carbon nanotubes for olive mill wastewater. *Polymers* 14 (3), 457. doi:10.3390/polym14030457

Ahmad, D., van den Boogaert, I., Miller, J., Presswell, R., and Jouhara, H. (2018). Hydrophilic and hydrophobic materials and their applications. *Energy Sources, Part A Recovery, Util. Environ. Eff.* 40 (22), 2686–2725. doi:10.1080/15567036.2018.1511642

Akram, Z., Aati, S., Ngo, H., and Fawzy, A. (2021). pH-dependent delivery of chlorhexidine from PGA grafted mesoporous silica nanoparticles at resin-dentin interface. *J. Nanobiotechnology* 19 (1), 43. doi:10.1186/s12951-021-00788-6

Al-Jaroudi, S., Ul-Hamid, A., Mohammed, A.-R., and Saner, S. (2007). Use of X-ray powder diffraction for quantitative analysis of carbonate rock reservoir samples. *Powder Technol. - POWDER Technol.* 175, 115–121. doi:10.1016/j.powtec.2007.01.013

Annane, K., Lemlikchi, W., and Tingry, S. (2021). Efficiency of eggshell as a low-cost adsorbent for removal of cadmium: kinetic and isotherm studies. *Biomass Convers. Biorefinery* 13, 6163–6174. doi:10.1007/s13399-021-01619-2

Aslam Khan, M. U., Al-Arjan, W. S., Binkadem, M. S., Mehboob, H., Haider, A., Raza, M. A., et al. (2021). Development of biopolymeric hybrid scaffold-based on AAc/GO/nHAp/TiO(2) nanocomposite for bone tissue engineering: *in-vitro* analysis. *Nanomater. (Basel, Switz.* 11 (5), 1319. doi:10.3390/nano11051319

Bhardwaj, S. B., Mehta, M., and Sood, S. (2020). Enterococci in the oral cavity of periodontitis patients from different urban socioeconomic groups. *Dent. Res. J.* 17 (2), 147–151. doi:10.4103/1735-3327.280894

Bokhari, N., Fatima, T., Nosheen, S., Iqbal, F., Moeen, F., and Sharif, F. (2023a). Bioactive bacterial cellulose–chitosan composite scaffolds for prospective periodontal tissue regeneration. *J. Mater. Res.* 38 (7), 1952–1962. doi:10.1557/s43578-023-00930-0

Bokhari, N., Yasmeen, A., Ali, A., Khalid, H., Wang, R., Bashir, M., et al. (2023b). Silk meshes coated with chitosan-bioactive phytochemicals activate wound healing genes *in vitro*. *Macromol. Biosci.* 23 (9), 2300039. doi:10.1002/mabi.202300039

Brum, I. S., Elias, C. N., Carvalho, J. J., Pires, J. L. S., Pereira, M. J. S., and Biasi, R. S., Properties of a bovine collagen type I membrane for guided bone regeneration applications, *e-Polymers*, 2021;21(1):210–221. doi:10.1515/epoly-2021-0021

Cannella, V., Altomare, R., Chiaramonte, G., Di Bella, S., Mira, F., Russotto, L., et al. (2019a). Cytotoxicity evaluation of endodontic pins on L929 cell line. *BioMed Res. Int.* 2019, 1–5. doi:10.1155/2019/3469525

Cannella, V., Altomare, R., Chiaramonte, G., Di Bella, S., Mira, F., Russotto, L., et al. (2019b). Cytotoxicity evaluation of endodontic pins on L929 cell line. *Biomed. Res. Int.* 2019, 1–5. doi:10.1155/2019/3469525

Dimitriou, R., Mataliotakis, G., Calori, G., and Giannoudis, P. (2012). The role of barrier membranes for guided bone regeneration and restoration of large bone defects: current experimental and clinical evidence. *BMC Med.* 10, 81. doi:10.1186/1741-7015-10-81

Dimitrov, I., and Tsvetanov, C. B. (2012). "4.27 - oligomeric Poly(ethylene oxide)s. Functionalized Poly(ethylene glycol)s. PEGylation," in *Polymer science: a comprehensive reference*. Editors K. Matyjaszewski and M. Möller (Amsterdam, Netherlands: Elsevier), 679–693.

Ensing, B., Tiwari, A., Tros, M., Hunger, J., Domingos, S. R., Pérez, C., et al. (2019). On the origin of the extremely different solubilities of polyethers in water. *Nat. Commun.* 10 (1), 2893. doi:10.1038/s41467-019-10783-z

Farahana, R. N., Supri, A. G., and Teh, P. I. (2015). Tensile and water absorption properties of eggshell powder filled recycled high-density polyethylene/ethylene vinyl acetate composites: effect of 3-aminopropyltriethoxysilane. *J. Adv. Res. Mater. Sci.* 5 (1), 1–9.

Fernandes, R. C., Damasceno, M. I., Pimentel, G., Mendonça, J. S., Gelfuso, M. V., da Silva Pereira, S. R. L., et al. (2020). Development of a membrane for guided tissue regeneration: an *in vitro* study. *Indian J. Dent. Res.* 31 (5), 763–767. doi:10.4103/ijdr.ijdr_244_19

Gao, Y., Wang, S., Shi, B., Wang, Y., Chen, Y., Wang, X., et al. (2022). Advances in modification methods based on biodegradable membranes in guided bone/tissue regeneration: a review. *Polym. (Basel)* 14 (5), 871. doi:10.3390/polym14050871

Geão, C., Costa-Pinto, A. R., Cunha-Reis, C., Ribeiro, V. P., Vieira, S., Oliveira, J. M., et al. (2019). Thermal annealed silk fibroin membranes for periodontal guided tissue regeneration. *J. Mater. Sci. Mater. Med.* 30 (2), 27. doi:10.1007/s10856-019-6225-y

Ghafoor, B., Ali, M. N., and Riaz, Z. (2020). Synthesis and appraisal of natural drug-polymer-based matrices relevant to the application of drug-eluting coronary stent coatings. *Cardiol. Res. Pract.* 2020, 4073091–4073111. doi:10.1155/2020/4073091

Ghosal, K., Chandra, A., Roy, S., Agatemor, C., Agatemor, C., et al. (2018). Electrospinning over solvent casting: tuning of mechanical properties of membranes. *Sci. Rep.* 8 (1), 5058. doi:10.1038/s41598-018-23378-3

Golińska, P. (2021). "Chapter 17 - biopolymer-based nanofilms: utility and toxicity," in *Biopolymer-based nano films*. Editors M. Rai and C. A. dos Santos (Amsterdam, Netherlands: Elsevier), 353–385.

Grundke, K., Pöschel, K., Synytska, A., Frenzel, R., Drechsler, A., Nitschke, M., et al. (2015). Experimental studies of contact angle hysteresis phenomena on polymer surfaces – toward the understanding and control of wettability for different applications. *Adv. colloid interface Sci.* 222, 350–376. doi:10.1016/j.cis.2014.10.012

He, P., Li, Y., Huang, Z., Guo, Z.-Z., Luo, B., Zhou, C.-R., et al. (2019). A multifunctional coaxial fiber membrane loaded with dual drugs for guided tissue regeneration. *J. Biomaterials Appl.* 34 (8), 1041–1051. doi:10.1177/0885328219894001

He, X.-T., Wu, R.-X., and Chen, F.-M. (2020). "Chapter 66 - periodontal tissue engineering and regeneration," in *Principles of tissue engineering*, R. Lanza, R. Langer, J. P. Vacanti, and A. Atala, (Cambridge, Massachusetts, United States: Academic Press), 1221–1249.

Joy Sinha, D., Jaiswal, N., Vasudeva, A., Prabha Tyagi, S., and Pratap Singh, U. (2017). Antibacterial effect of Azadirachta indica (neem) or curcuma longa (turmeric) against *Enterococcus faecalis* compared with that of 5% sodium hypochlorite or 2% chlorhexidine *in vitro*. *Bull. Tokyo Dent. Coll.* 58 (2), 103–109. doi:10.2209/tdcpublication.2015-0029

Khan, M. U. A., Razak, S. I. A., Haider, S., Mannan, H. A., Hussain, J., and Hasan, A. (2022a). Sodium alginate-f-GO composite hydrogels for tissue regeneration and antitumor applications. *Int. J. Biol. Macromol.* 208, 475–485. doi:10.1016/j.ijbiomac.2022.03.091

Khan, M. U. A., Razak, S. I. A., Rehman, S., Hasan, A., Qureshi, S., and Stojanović, G. M. (2022c). Bioactive scaffold (sodium alginate)-g-(nHAp@SiO2@GO) for bone tissue engineering. *Int. J. Biol. Macromol.* 222, 462–472. doi:10.1016/j.ijbiomac.2022.09.153

Khan, M. U. A., Rizwan, M., Razak, S. I. A., Hassan, A., Rasheed, T., and Bilal, M. (2022b). Electroactive polymeric nanocomposite BC-g-(Fe(3)O(4)/GO) materials for bone tissue engineering: *in vitro* evaluations. *J. biomaterials Sci. Polym. Ed.* 33 (11), 1349–1368. doi:10.1080/09205063.2022.2054544

Latthe, S., Terashima, C., Nakata, K., and Fujishima, A. (2014). Superhydrophobic surfaces developed by mimicking hierarchical surface morphology of Lotus leaf. *Mol. (Basel, Switz.* 19, 4256–4283. doi:10.3390/molecules19044256

Lenzi, T. L., Tedesco, T. K., Soares, F. Z., Loguercio, A. D., and Rocha Rde, O. (2012). Chlorhexidine does not increase immediate bond strength of etch-and-rinse adhesive to caries-affected dentin of primary and permanent teeth. *Braz. Dent. J.* 23 (4), 438–442. doi:10.1590/s0103-64402012000400022

Li, L., Crosby, K., and Sawicki, M. (2012). Effects of surface roughness of hydroxyapatite on cell attachment and proliferation. *J. Biotechnol. Biomaterials* 02. doi:10.4172/2155-952x.1000150

Liu, J. X., Werner, J., Kirsch, T., Zuckerman, J. D., and Virk, M. S. (2018). Cytotoxicity evaluation of chlorhexidine gluconate on human fibroblasts, myoblasts, and osteoblasts. *J. bone Jt. Infect.* 3 (4), 165–172. doi:10.7150/jbji.26355

Lopez-Berganza, J. A., Song, R., Elbanna, A., and Espinosa-Marzal, R. M. (2017). Calcium carbonate with nanogranular microstructure yields enhanced toughness. *Nanoscale* 9 (43), 16689–16699. doi:10.1039/c7nr05347a

Mahapatro, A., and Singh, D. (2011). Biodegradable nanoparticles are excellent vehicle for site directed *in-vivo* delivery of drugs and vaccines. *J. nanobiotechnology* 9, 55. doi:10.1186/1477-3155-9-55

Masoudi Rad, M., Nouri Khorasani, S., Ghasemi-Mobarakeh, L., Prabhakaran, M. P., Foroughi, M. R., Kharaziha, M., et al. (2017). Fabrication and characterization of two-layered nanofibrous membrane for guided bone and tissue regeneration application. *Mater. Sci. Eng. C, Mater. Biol. Appl.* 80, 75–87. doi:10.1016/j.msec.2017.05.125

McGauran, T., Dunne, N., Smyth, B. M., and Cunningham, E. (2020). Incorporation of poultry eggshell and litter ash as high loading polymer fillers in polypropylene. *Compos. Part C. Open Access* 3, 100080. doi:10.1016/j.jcomc.2020.100080

Milella, E., Ramires, P. A., Brescia, E., La Sala, G., Paola, L., and Bruno, V. (2001). Physicochemical, mechanical, and biological properties of commercial membranes for GTR. *J. Biomed. Mater. Res.* 58, 427–435. doi:10.1002/jbm.1038

Navarro, J., Swayambunathan, J., Lerman, M., Santoro, M., and Fisher, J. P. (2019). Development of keratin-based membranes for potential use in skin repair. *Acta biomater.* 83, 177–188. doi:10.1016/j.actbio.2018.10.025

Poppolo Deus, F., and Ouanounou, A. (2022). Chlorhexidine in dentistry: pharmacology, uses, and adverse effects. *Int. Dent. J.* 72 (3), 269–277. doi:10.1016/j.identj.2022.01.005

Priyadarshini, B. M., Selvan, S. T., Narayanan, K., and Fawzy, A. S. (2017). Characterization of chlorhexidine-loaded calcium-hydroxide microparticles as a potential dental pulp-capping material. *Mater. Bioeng. (Basel, Switz.* 4 (3), 59. doi:10.3390/bioengineering4030059

Qasim, S. S. B., Baig, M. R., Matinlinna, J. P., Daood, U., and Al-Asfour, A. (2021a). Highly segregated biocomposite membrane as a functionally graded template for periodontal tissue regeneration. *Membranes* 11 (9), 667. doi:10.3390/membranes11090667

Qasim, S. S. B., Baig, M. R., Matinlinna, J. P., Daood, U., and Al-Asfour, A. (2021b). Highly segregated biocomposite membrane as a functionally graded template for periodontal tissue regeneration. *Membr. (Basel).* 11 (9), 667. doi:10.3390/membranes11090667

Reddy, M. S., Ponnamma, D., Choudhary, R., and Sadasivuni, K. K. (2021). A comparative review of natural and synthetic biopolymer composite scaffolds. *Polymers* 13 (7), 1105. doi:10.3390/polym13071105

Rondon, E. P., Benabdoun, H. A., Vallières, F., Segalla Petrônio, M., Tiera, M. J., Benderdour, M., et al. (2020). Evidence supporting the safety of pegylated diethylaminoethyl-chitosan polymer as a nanovector for gene therapy applications. *Int. J. nanomedicine* 15, 6183–6200. doi:10.2147/ijn.s252397

Rudolf, J. L., Moser, C., Sculean, A., and Eick, S. (2019). *In-vitro* antibiofilm activity of chlorhexidine digluconate on polylactide-based and collagen-based membranes. *BMC oral health* 19 (1), 291. doi:10.1186/s12903-019-0979-y

Sam, G., Vadakkekuttical, R. J., and Amol, N. V. (2015). *In vitro* evaluation of mechanical properties of platelet-rich fibrin membrane and scanning electron microscopic examination of its surface characteristics. *J. Indian Soc. Periodontology* 19 (1), 32–36. doi:10.4103/0972-124x.145821

Shamsuri, A. A., and Sumadin, Z. A. (2018). Influence of hydrophobic and hydrophilic mineral fillers on processing, tensile and impact properties of LDPE/KCF biocomposites. *Compos. Commun.* 9, 65–69. doi:10.1016/j.coco.2018.06.003

Shiferaw, N., Habte, L., Thenepalli, T., and Ahn, J. W. (2019). Effect of eggshell powder on the hydration of cement paste. *Mater. (Basel, Switz.* 12 (15), 2483. doi:10.3390/ma12152483

Skórczewska, K., Lewandowski, K., Szewczykowski, P., Wilczewski, S., Szulc, J., Stopa, P., et al. (2022). Waste eggshells as a natural filler for the poly(vinyl chloride) composites. *Polymers* 14 (20), 4372. doi:10.3390/polym14204372

Soltani Dehnavi, S., Mehdikhani, M., Rafienia, M., and Bonakdar, S. (2018). Preparation and *in vitro* evaluation of polycaprolactone/PEG/bioactive glass nanopowders nanocomposite membranes for GTR/GBR applications. *Mater. Sci. Eng. C* 90, 236–247. doi:10.1016/j.msec.2018.04.065

Sunandhakumari, V. J., Vidhyadharan, A. K., Alim, A., Kumar, D., Ravindran, J., Krishna, A., et al. (2018). Fabrication and *in vitro* characterization of bioactive glass/nano hydroxyapatite reinforced electrospun poly(ε-caprolactone) composite membranes for guided tissue regeneration. *Bioeng. (Basel)* 5 (3), 54. doi:10.3390/bioengineering5030054

Susanto, A., Satari, M., Abbas, B., Koesoemowidodo, R., and Cahyanto, A. (2019). Fabrication and characterization of chitosan-collagen membrane from barramundi (Lates calcarifer) scales for guided tissue regeneration. *Eur. J. Dent.* 13, 370–375. doi:10.1055/s-0039-1698610

Thangavelu, A., Kaspar, S., Kathirvelu, R., Srinivasan, B., Srinivasan, S., and Chlorhexidine, S. R. (2020). Chlorhexidine: an elixir for periodontics. *elixir periodontics* 12 (5), 57–59. doi:10.4103/jpbs.jpbs_162_20

Thomas, N. G., Sanil, G. P., Gopimohan, R., Prabhakaran, J. V., Thomas, G., and Panda, A. K. (2012). Biocompatibility and cytotoxic evaluation of drug-loaded biodegradable guided tissue regeneration membranes. *J. Indian Soc. Periodontology* 16 (4), 498–503. doi:10.4103/0972-124x.106883

Vasudevan, G., and Chan Wei, S. (2020). Utilisation of eggshell powder (ESP) as partial replacement of cement incorporating superplasticizer. *IOP Conf. Ser. Mater. Sci. Eng.* 840 (1), 012016. doi:10.1088/1757-899x/840/1/012016

Wang, J., Wang, L., Zhou, Z., Lai, H., Xu, P., Liao, L., et al. (2016). Biodegradable polymer membranes applied in guided bone/tissue regeneration: a review. *Polymers* 8 (4), 115. doi:10.3390/polym8040115

Wei, H., Shen, Q., Zhao, Y., Wang, D., Xu, D., and Schieber, M. (2004). "Crystallization habit of calcium carbonate in the presence of sodium dodecyl sulfate and/or polypyrrolidone". *J. Cryst. Growth*, 26010. doi:10.1016/j.jcrysgro.2003.08.047

Wu, Y., Chen, S., Luo, P., Deng, S., Shan, Z., Fang, J., et al. (2022). Optimizing the biodegradability and biocompatibility of a biogenic collagen membrane through cross-linking and zinc-doped hydroxyapatite. *Acta Biomater.* 143, 159–172. doi:10.1016/j.actbio.2022.02.004

Yang, Z., Wu, C., Shi, H., Luo, X., Sun, H., Wang, Q., et al. (2022). Advances in barrier membranes for guided bone regeneration techniques. *Front. Bioeng. Biotechnol.* 10, 921576. doi:10.3389/fbioe.2022.921576

Zehra, A., Bokhari, N., Nosheen, S., Bashir, M., Khan, A., Khan, F. A., et al. (2023). Electrospun bilayer membranes carrying bearberry/licorice extract to ameliorate wound healing. *J. Polym. Environ.*, doi:10.1007/s10924-023-03007-5

Zhang, K., Zhao, M., Cai, L., Wang, Z.-k., Sun, Y.-f., and Hu, Q.-l. (2010). Preparation of chitosan/hydroxyapatite guided membrane used for periodontal tissue regeneration. *Chin. J. Polym. Sci.* 28 (4), 555–561. doi:10.1007/s10118-010-9087-9

Zimina, A., Senatov, F., Choudhary, R., Kolesnikov, E., Anisimova, N., Kiselevskiy, M., et al. (2020). Biocompatibility and physico-chemical properties of highly porous PLA/HA scaffolds for bone reconstruction. *Bone Reconstr.* 12 (12), 2938. doi:10.3390/polym12122938